

LoRa Symbol Error Rate Under Non-Chip- and Non-Phase-Aligned Interference

Orion Afisiadis, Matthieu Cotting, Andreas Burg, and Alexios Balatsoukas-Stimming

Telecommunication Circuits Laboratory
École polytechnique fédérale de Lausanne, Switzerland
Email: orion.afisiadis@epfl.ch

Abstract—In this work, we examine the performance of the LoRa chirp spread spectrum modulation in the presence of both additive white Gaussian noise and interference from another LoRa user. To this end, we extend an existing interference model to the more realistic case where the interfering user is neither chip- nor phase-aligned with the signal of interest and we derive an expression for the SER. We show that the existing interference model overestimates the effect of interference on the error rate. Moreover, we derive a low-complexity approximate formula that can significantly reduce the complexity of computing the symbol error rate compared to the complete expression.

I. INTRODUCTION

LoRa is a low-rate, low-power, and high-range modulation that uses chirp spread-spectrum for its physical layer [1]. LoRa supports multiple spreading factors, coding rates, and packet lengths, to support a wide range of operating signal-to-noise ratios (SNRs). The LoRa physical layer is proprietary, but reverse engineering attempts that have been carried out [2], [3] have revealed the mathematical description [4]. The effect of carrier- and sampling-frequency offset on LoRa digital receivers has been modeled and analyzed in [5]. For MAC layer, LoRa relies on LoRaWAN, which uses an ALOHA-based mechanism, meaning that collisions are not explicitly avoided and that the scalability of the network is potentially limited by inter-node interference [6], [7]. An overview and performance evaluations of LoRaWAN can be found in [7].

Since LoRa uses the ISM band, interference from other technologies using the same band is another potential problem and has received some attention in the literature. Specifically, [8] studies the co-existence of LoRa with IEEE 802.15.4g, while [9] studies the co-existence of LoRa with ultra-narrowband technologies, such as Sigfox. The impact of interference coming from other LoRa nodes has also received some attention. Specifically, the work of [10] examines the effect of imperfect orthogonality between different LoRa spreading factors by examining the signal-to-interference ratio (SIR) threshold for receiving a packet correctly for all combinations of spreading factors. However, interference is particularly detrimental when users with the same spreading factor collide. The authors of [11] perform an experimental assessment of the link-level characteristics of the LoRa system, followed by a system-level simulation to assess the capacity of a LoRaWAN network. Convenient approximate formulas for the bit-error rate (BER) of the LoRa modulation when transmission takes place over additive white Gaussian noise

(AWGN) and Rayleigh fading channels are given in [12] but collisions are not considered. Finally, the work of [13], which is most closely related to our work, provides an approximation for the BER of the LoRa modulation under AWGN and interference from a single LoRa interferer with the same spreading factor (*same-SF*). Capacity planning for LoRa with the aforementioned interference model is addressed in [14].

Contributions: The work of [13] made a significant first step toward understanding of the behavior of LoRa under same-SF interference. In this work, we extend the interference model of [13] to the more general (and more realistic) case where the interference is neither chip- nor phase-aligned with the signal-of-interest. We derive an expression for the symbol-error rate (SER) under this new complete interference model. Moreover, we derive an approximation for the SER under the new interference model and we show that non-integer chip duration time-misalignment in particular has a significant effect on the SER. Specifically, we show that the interference model of [13] is pessimistic in the sense that it consistently over-estimates the actual SER.

II. THE LORA MODULATION

LoRa is a spread-spectrum modulation that uses a bandwidth B and $N = 2^{\text{SF}}$ chips per symbol, where SF is called the *spreading factor* with $\text{SF} \in \{7, \dots, 12\}$. When considering the discrete-time baseband equivalent signal, the bandwidth B is split into N frequency steps. A symbol $s \in \mathcal{S}$, where $\mathcal{S} = \{0, \dots, N-1\}$, begins at frequency $(\frac{sB}{N} - \frac{B}{2})$. The frequency increases by $\frac{B}{N}$ at each chip until it reaches the Nyquist frequency $\frac{B}{2}$. When the Nyquist frequency is reached, there is a frequency fold to $-\frac{B}{2}$ at chip $n_{\text{fold}} = N - s$. The general discrete-time baseband equivalent description of a LoRa symbol s is

$$x_s[n] = \begin{cases} e^{j2\pi\left(\frac{1}{2N}\left(\frac{B}{f_s}\right)^2 n^2 + \left(\frac{s}{N} - \frac{1}{2}\right)\left(\frac{B}{f_s}\right)n\right)}, & n \in \mathcal{S}_1 \\ e^{j2\pi\left(\frac{1}{2N}\left(\frac{B}{f_s}\right)^2 n^2 + \left(\frac{s}{N} - \frac{3}{2}\right)\left(\frac{B}{f_s}\right)n\right)}, & n \in \mathcal{S}_2, \end{cases} \quad (1)$$

where $\mathcal{S}_1 = \{0, \dots, n_{\text{fold}} - 1\}$ and $\mathcal{S}_2 = \{n_{\text{fold}}, \dots, N - 1\}$. In the practically relevant case where the sampling frequency f_s is equal to B , which we assume for the remainder of this manuscript, the discrete-time baseband equivalent equation of a LoRa symbol s can be simplified to

$$x_s[n] = e^{j2\pi\left(\frac{n^2}{2N} + \left(\frac{s}{N} - \frac{1}{2}\right)n\right)}, \quad n \in \mathcal{S}. \quad (2)$$

After transmission over a time-invariant and frequency-flat wireless channel with complex-valued channel gain $h \in \mathbb{C}$, the received LoRa symbol is given by

$$y[n] = hx_s[n] + z[n], \quad n \in \mathcal{S}, \quad (3)$$

where $z[n] \sim \mathcal{CN}(0, \sigma^2)$ is complex additive white Gaussian noise with $\sigma^2 = \frac{N_0}{N}$ and N_0 is the singled-sided noise power spectral density. We assume that $|h| = 1$ without loss of generality, so that the signal-to-noise ratio (SNR) is $\frac{1}{N_0}$.

To demodulate the symbols, first a *dechirping* is performed, where the received signal is multiplied by the complex conjugate of a reference signal x_{ref} . A convenient choice for this reference signal is an *upchirp*, i.e., the LoRa symbol for $s = 0$

$$x_{\text{ref}}[n] = e^{j2\pi\left(\frac{\sigma^2}{2N}n - \frac{\sigma^2}{2}\right)}, \quad n \in \mathcal{S}. \quad (4)$$

Then, the non-normalized discrete Fourier transform (DFT) is applied to the dechirped signal in order to obtain $\mathbf{Y} = \text{DFT}(\mathbf{y} \odot \mathbf{x}_{\text{ref}}^*)$, where \odot denotes the Hadamard product and $\mathbf{y} = [y[0] \dots y[N-1]]$ and $\mathbf{x}_{\text{ref}} = [x_{\text{ref}}[0] \dots x_{\text{ref}}[N-1]]$. Demodulation can be performed by selecting the bin index with the maximum magnitude

$$\hat{s} = \arg \max_{k \in \mathcal{S}} (|Y_k|). \quad (5)$$

III. SYMBOL ERROR RATE UNDER AWGN

In this section, we first derive the expression for the LoRa SER under additive white Gaussian noise (AWGN), which is useful for later explaining how the SER can be calculated in the presence of both AWGN and interference.

A. Distribution of the Decision Metric

In the absence of noise, and with perfect synchronization, the DFT of the dechirped signal \mathbf{Y} has a single frequency bin that contains all the signal energy (i.e., a bin with magnitude N) and all remaining $N - 1$ bins have zero energy. On the other hand, when AWGN is present, all frequency bins will contain some energy. The distribution of the frequency bin values Y_k for $k \in \mathcal{S}$ is

$$Y_k \sim \begin{cases} \mathcal{CN}(0, \sigma^2), & k \in \mathcal{S}/s \\ \mathcal{CN}(N(\cos \phi + j \sin \phi), \sigma^2), & k = s, \end{cases} \quad (6)$$

where $\phi = \angle h$ denotes a phase shift introduced by the transmission channel h that is fixed for each transmission but generally uniformly distributed in $[0, 2\pi)$ and s is the transmitted symbol.

Let us define $Y'_k = \frac{Y_k}{\sigma}$ for $k \in \mathcal{S}$. The values Y'_k can be used in (5) instead of Y_k without changing the result and their distribution is

$$Y'_k \sim \begin{cases} \mathcal{CN}(0, 1), & k \in \mathcal{S}/s \\ \mathcal{CN}\left(\frac{N \cos \phi}{\sigma} + j \frac{N \sin \phi}{\sigma}, 1\right), & k = s. \end{cases} \quad (7)$$

Using basic properties of the complex normal distribution, we can show that the demodulation metric $|Y'_k|$ follows a Rayleigh distribution for $k \in \mathcal{S}/s$ and a Rice distribution for $k = s$

$$|Y'_k| \sim \begin{cases} f_{\text{Ra}}(y; 1), & k \in \mathcal{S}/s \\ f_{\text{Ri}}\left(y; \frac{N}{\sigma}, 1\right), & k = s. \end{cases} \quad (8)$$

We denote the probability density function (PDF) and the cumulative density function (CDF) of the Rayleigh and Rice distributions by $f_{\text{Ra}}(y; \sigma)$, $f_{\text{Ri}}(y; v, \sigma)$ and $F_{\text{Ra}}(y; \sigma)$, $F_{\text{Ri}}(y; v, \sigma)$, respectively, where σ and v denote the *scale* and *location* parameters.

B. Symbol Error Rate

A symbol error occurs if and only if any of the $|Y'_k|$ values for $k \in \mathcal{S}/s$ exceeds the value of $|Y'_s|$, or, equivalently, if and only if $|Y'_{\text{max}}| > |Y'_s|$, where $|Y'_{\text{max}}| = \max_{k \in \mathcal{S}/s} |Y'_k|$. Using order statistics [15] and the fact that all $|Y'_k|$ for $k \in \mathcal{S}/s$ are i.i.d., the PDF of $|Y'_{\text{max}}|$ can be obtained as

$$f_{|Y'_{\text{max}}|}(y) = (N - 1) f_{\text{Ra}}(y; 1) F_{\text{Ra}}(y; 1)^{(N-2)} \quad (9)$$

Using $f_{|Y'_{\text{max}}|}(y)$, the conditional SER when symbol s is transmitted can be calculated as

$$P(\hat{s} \neq s | s) = \int_{y=0}^{+\infty} \int_{x=0}^y f_{\text{Ri}}(x; v, 1) f_{|Y'_{\text{max}}|}(y) dx dy \quad (10)$$

$$= \int_{y=0}^{+\infty} F_{\text{Ri}}(y; v, 1) f_{|Y'_{\text{max}}|}(y) dy, \quad (11)$$

with $v = \frac{N}{\sigma}$. The SER for all symbols s is identical, meaning that (11) is in fact equal to the average SER and, if we assume that all symbols are equiprobable, also the expected SER.

C. Symbol Error Rate Approximations

While the evaluation of (11) is in principle straightforward, in practice the values of N in the LoRa modulation are very large so that numerical problems arise. For this reason, two approximations that can be used to efficiently evaluate (11) were derived in [12]. Specifically, [12] used a Gaussian approximation so that $|Y'_s| \sim \mathcal{N}\left(\frac{N}{\sigma}, 1\right)$ and $|Y'_{\text{max}}| \sim \mathcal{N}\left(\mu_\beta, \sigma_\beta^2\right)$ and where appropriate expressions are given to calculate μ_β and σ_β^2 . With our definition of the SNR, the SER can be calculated as

$$P(\hat{s} \neq s) \approx Q\left(\frac{\sqrt{\text{SNR}} - \left((H_{N-1})^2 - \frac{\pi^2}{12}\right)^{1/4}}{\sqrt{H_{N-1} - \sqrt{(H_{N-1})^2 - \frac{\pi^2}{12} + 0.5}}}\right), \quad (12)$$

where $H_n = \sum_{k=1}^n \frac{1}{k}$ denotes the n th harmonic number and $Q(\cdot)$ denotes the Q-function.

IV. SYMBOL ERROR RATE UNDER AWGN AND SAME-SF LORA INTERFERENCE

In this section, we analyze the case of a gateway trying to decode the message of a user in the presence of an interfering LoRa device, as depicted in Fig. 1. We assume that the LoRa gateway is perfectly synchronized to the user whose message is decoded. Various synchronization techniques for LoRa have been explained in the literature [3]. It has been shown that interferers with different spreading factors can be considered approximately orthogonal [16], [17]. Therefore, in this work we limit our model to interference signals with the same spreading factor as the one employed by the user. Finally,

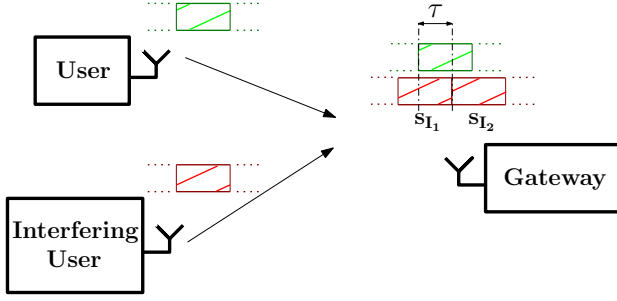


Fig. 1. Illustration of LoRa uplink transmission with one interfering user having an arbitrary τ .

for simplicity, in this work we only consider one interfering user. In this case, the general signal model is

$$y[n] = hx[n] + h_I x_I[n] + z[n], \quad n \in \mathcal{S}, \quad (13)$$

where h is the channel gain between the user of interest and the LoRa gateway, $x[n]$ is the signal of interest, h_I is the channel gain between the interferer and the LoRa gateway, $x_I[n]$ is the interfering signal, and $z[n] \sim \mathcal{N}(0, \sigma^2)$ is additive white Gaussian noise. Since we assume that $|h| = 1$, the signal-to-interference ratio (SIR) can be defined as

$$\text{SIR} = \frac{1}{|h_I|^2} = \frac{1}{P_I}, \quad (14)$$

where we use P_I to denote the power of the interfering user. Since LoRa uses the (non-slotted) ALOHA protocol for medium access control, the interfering signal $y_I[n] = h_I x_I[n]$ is not synchronized in any way to the user or the gateway. Due to the lack of synchronization, the interfering signal $x_I[n]$ will generally be a combination of parts of two distinct LoRa symbols, which we denote by s_{I_1} and s_{I_2} , as shown in Fig. 1.

Let τ denote the relative time-offset between the first chip of the symbol of interest s and the first chip of the interfering symbol s_{I_2} (i.e., the first chip of the interfering symbol s_{I_2} starts τ chip durations *after* the first chip of s). Due to the complete lack of synchronization, we assume that τ is uniformly distributed in $[0, N]$. We note that in [13], the offset τ is constrained to integer chip durations, which is not particularly realistic since it effectively assumes that the interferer is chip-aligned with the user. Let $\mathcal{N}_{L_1} = \{0, \dots, \lceil \tau \rceil - 1\}$ and $\mathcal{N}_{L_2} = \{\lceil \tau \rceil, \dots, N - 1\}$. The discrete-time baseband equivalent equation of $x_I[n]$ can be found using (2) for s_{I_1} and s_{I_2} , appropriately adjusted to include the offset τ

$$x_I[n] = \begin{cases} e^{j2\pi \left(\frac{(n+N-\tau)^2}{2N} + (n+N-\tau) \left(\frac{s_{I_1}}{N} - \frac{1}{2} \right) \right)}, & n \in \mathcal{N}_{L_1} \\ e^{j2\pi \left(\frac{(n-\tau)^2}{2N} + (n-\tau) \left(\frac{s_{I_2}}{N} - \frac{1}{2} \right) \right)}, & n \in \mathcal{N}_{L_2}. \end{cases} \quad (15)$$

The demodulation of $y[n]$ at the receiver yields

$$\begin{aligned} \mathbf{Y} &= \text{DFT}(\mathbf{y} \odot \mathbf{x}_{\text{ref}}^*) \\ &= \text{DFT}(h\mathbf{x} \odot \mathbf{x}_{\text{ref}}^*) + \text{DFT}(h_I \mathbf{x}_I \odot \mathbf{x}_{\text{ref}}^*) + \text{DFT}(\mathbf{z} \odot \mathbf{x}_{\text{ref}}^*). \end{aligned} \quad (16)$$

$$(17)$$

We call $\text{DFT}(\mathbf{x}_I \odot \mathbf{x}_{\text{ref}}^*)$ and $\text{DFT}(h_I \mathbf{x}_I \odot \mathbf{x}_{\text{ref}}^*) = \text{DFT}(\mathbf{y}_I \odot \mathbf{x}_{\text{ref}}^*)$ the transmitted and received *interference patterns*, respectively. It is clear that the interference pattern depends on the time-domain interference signal \mathbf{y}_I , which is in turn a function of the interfering symbols s_{I_1} , s_{I_2} , the channel h_I , and the interferer time-offset τ .

A. Distribution of the Decision Metric

Let R_k denote the value of the transmitted interference pattern at frequency bin k , i.e.,

$$R_k = \text{DFT}(\mathbf{x}_I \odot \mathbf{x}_{\text{ref}}^*)[k], \quad k \in \mathcal{S}. \quad (19)$$

For a specific combination of a symbol s and an interference pattern \mathbf{y}_I , adding the interference to the signal of interest corresponds to changing the mean value of the distribution of Y'_k in (7), as follows:

$$Y'_k \sim \begin{cases} \mathcal{CN} \left(\frac{|h_I R_k| \cos \theta}{\sigma} + j \frac{|h_I R_k| \sin \theta}{\sigma}, 1 \right), & k \in \mathcal{S}/s \\ \mathcal{CN} \left(\frac{N \cos \phi + |h_I R_k| \cos \theta}{\sigma} + j \frac{N \sin \phi + |h_I R_k| \sin \theta}{\sigma}, 1 \right), & k = s, \end{cases} \quad (20)$$

where $\theta = \angle h_I$ is the phase shift introduced by the interference channel and is fixed for each transmission but generally uniformly distributed in $[0, 2\pi)$. Thus, in the presence of interference, the demodulation metric $|Y'_k|$ used in (5) is distributed according to

$$|Y'_k| \sim \begin{cases} f_{\text{Ri}} \left(y; \frac{|h_I R_k|}{\sigma}, 1 \right), & k \in \mathcal{S}/s \\ f_{\text{Ri}} \left(y; \frac{\sqrt{N^2 + |h_I R_k|^2 + 2N|h_I R_k| \cos(\omega)}}{\sigma}, 1 \right), & k = s, \end{cases} \quad (21)$$

where we define the phase shift between the user and the interfering user as $\omega = \phi - \theta$ for simplicity.

B. Symbol Error Rate

Similarly to (11), in the presence of interference the SER conditioned on s , \mathbf{y}_I , and ω , can be written as

$$P(\hat{s} \neq s | s, \mathbf{y}_I, \omega) = 1 - \int_{y=0}^{+\infty} f_{\text{Ri}}(y; v_s, 1) F_{|Y'_{\max}|}(y) dy, \quad (22)$$

where $v_s = \frac{1}{\sigma} \sqrt{N^2 + |h_I R_s|^2 + 2N|h_I R_s| \cos(\omega)}$ is the location parameter for the bin $k = s$. The CDF of the N th order statistic is known to be $F_n(x) = P(X_1 < x)P(X_2 < x) \dots P(X_n < x)$. Thus, we can directly deduce that the CDF of the maximum interfering bin is

$$F_{|Y'_{\max}|}(y) = \prod_{\substack{k=1 \\ k \neq s}}^N F_{\text{Ri}}(y; v_k, 1), \quad (23)$$

where $v_k = \frac{|h_I R_k|}{\sigma}$. By taking the expectation of $P(\hat{s} \neq s | s, \mathbf{y}_I, \omega)$ with respect to ω , we get the SER conditioned on s , \mathbf{y}_I

$$P(\hat{s} \neq s | s, \mathbf{y}_I) = \frac{1}{2\pi} \int_{\omega=0}^{2\pi} P(\hat{s} \neq s | s, \mathbf{y}_I, \omega) d\omega. \quad (24)$$

$$P(\hat{s} \neq s) = 1 - \frac{1}{2\pi N^4} \sum_{s=0}^{N-1} \sum_{s_{I_1}=0}^{N-1} \sum_{s_{I_2}=0}^{N-1} \int_{\tau=0}^N \int_{\omega=0}^{2\pi} \int_{y=0}^{+\infty} f_{\text{Ri}}(y; v_s, 1) \prod_{\substack{k=1 \\ k \neq s}}^N F_{\text{Ri}}(y; v_k, 1) dy d\omega d\tau. \quad (18)$$

Recall that, by assumption, s_{I_1} and s_{I_2} are uniformly distributed in \mathcal{S} and τ is uniformly distributed in $[0, N)$. As such, the conditional SER $P(\hat{s} \neq s|s)$ can be computed as

$$P(\hat{s} \neq s|s) = \frac{1}{N^3} \sum_{s_{I_1}=0}^{N-1} \sum_{s_{I_2}=0}^{N-1} \int_0^N P(\hat{s} \neq s|s, \mathbf{y}_I) d\tau. \quad (25)$$

Finally, s is also uniformly distributed in \mathcal{S} , so that the unconditional SER becomes

$$P(\hat{s} \neq s) = \frac{1}{N} \sum_{s=0}^{N-1} P(\hat{s} \neq s|s). \quad (26)$$

The full expression for $P(\hat{s} \neq s)$ is given in (18).

V. SYMBOL ERROR RATE APPROXIMATION

Apart from the numerical problems that arise from the product of $(N-1)$ CDFs in (18), the computational complexity of evaluating (18) is very high. For this reason, in this section, we derive an approximation for (18).

A. Interference Patterns

We first derive an explicit form for the magnitude of the transmitted interference pattern R_k , $k \in \mathcal{S}$. Note that the offset τ can be split into an integer part L and a non-integer part λ , i.e., $L = \lfloor \tau \rfloor$, and $\lambda = \tau - \lfloor \tau \rfloor$. Using the definition of the DFT and after some algebraic transformations, we obtain

$$R_k = A_{k,1} e^{-j\theta_{k,1}} + A_{k,2} e^{-j\theta_{k,2}}, \quad (27)$$

where

$$A_{k,1} = \frac{\sin\left(\frac{\pi}{N}(s_{I_1} - k - \tau)\lceil\tau\rceil\right)}{\sin\left(\frac{\pi}{N}(s_{I_1} - k - \tau)\right)}, \quad (28)$$

$$A_{k,2} = \frac{\sin\left(\frac{\pi}{N}(s_{I_2} - k - \tau)(N - \lceil\tau\rceil)\right)}{\sin\left(\frac{\pi}{N}(s_{I_2} - k - \tau)\right)}, \quad (29)$$

and

$$\theta_{k,1} = \frac{\pi}{N} \left(-\tau^2 + (\lambda - L)N + s_{I_1}(2\tau - \lceil\tau\rceil + 1) + k(\lceil\tau\rceil - 1) + \tau(\lceil\tau\rceil - 1) \right), \quad (30)$$

$$\theta_{k,2} = \frac{\pi}{N} \left(-\tau^2 + s_{I_2}(2\tau - \lceil\tau\rceil + 1 - N) + k(\lceil\tau\rceil - 1 + N) + \tau(\lceil\tau\rceil - 1) \right). \quad (31)$$

We define $[x]_y = x \bmod y$. For the special case where τ is an integer and $k = [s_{I_1} - \tau]_N$ and $k = [s_{I_2} - \tau]_N$, (28) and (29), respectively, are of the indeterminate form $0/0$. Using L'Hôpital's rule, it can be shown that in these cases we have $A_{k,1} = \lceil\tau\rceil$, and $A_{k,2} = N - \lceil\tau\rceil$. The magnitude of R_k in (27) can be written as

$$|R_k| = \sqrt{A_{k,1}^2 + A_{k,2}^2 + 2A_{k,1}A_{k,2} \cos(\theta_{k,1} - \theta_{k,2})}. \quad (32)$$

B. Symbol Error Rate Approximation

We now follow a procedure that is similar to the procedure in [13] in order to derive a simple approximation for $P(\hat{s} \neq s)$ that is also more efficient to evaluate than (18). First, using the triangle inequality, we can simplify (32) to

$$|R_k| \approx |A_{k,1}| + |A_{k,2}|. \quad (33)$$

We assume that the interference-induced SER is dominated by the maximum of $|R_k|$. Thus, we are interested in evaluating

$$|R_{k_{\max}}| = \max_k (|A_{k,1}| + |A_{k,2}|). \quad (34)$$

Similarly to [13], we choose

$$k_{\max} \approx \arg \max_k (|A_{k,2}|) = \lfloor \tau \rfloor, \quad (35)$$

so that we can easily approximate R_{\max} as

$$|R_{k_{\max}}| \approx |A_{\lfloor \tau \rfloor, 1} + A_{\lfloor \tau \rfloor, 2}|. \quad (36)$$

The probability that the (maximum) interference bin $\lfloor \tau \rfloor$ coincides with the bin of the signal-of-interest s is $\frac{1}{N}$. Thus, for the approximation of the SER, we only consider the cases where $\lfloor \tau \rfloor \neq s$. Only considering $\lfloor \tau \rfloor \neq s$ also has the convenient side-effect that we ignore the only case of (21) which contains ω , meaning that we can entirely avoid the integration over ω in the computation of $P(\hat{s} \neq s|s, \mathbf{y}_I)$. Let $P^{(I)}(\hat{s} \neq s)$ denote the SER under interference resulting from the approximation in (36). As explained in Section IV-A, $|Y'_{k_{\max}}|$ follows a Rice distribution, which can be approximated by a Gaussian distribution for large location parameters [13] so that

$$|Y'_{k_{\max}}| \sim \mathcal{N}\left(\frac{|h_I||R_{k_{\max}}|}{\sigma}, 1\right). \quad (37)$$

Using the Gaussian approximation, $P^{(I)}(\hat{s} \neq s)$ is

$$P^{(I)}(\hat{s} \neq s) = \frac{1}{N^3} \sum_{s_{I_1}=0}^{N-1} \sum_{s_{I_2}=0}^{N-1} \int_0^N Q\left(\frac{N - |h_I||R_{\max}|}{\sqrt{2}\sigma^2}\right) d\tau, \quad (38)$$

where $Q(\cdot)$ denotes the Q-function and the integral can be evaluated numerically by discretizing the interval $[0, N)$ with a step size ϵ . In the AWGN-limited regime, the above approximation becomes inaccurate, since no single bin dominates the error rate. Let $P^{(N)}(\hat{s} \neq s)$ denote the SER under AWGN given in (11). Then, a final estimate of the SER that is more accurate also in the low SNR regime can be obtained as

$$P(\hat{s} \neq s) \approx P^{(N)}(\hat{s} \neq s) + (1 - P^{(N)}(\hat{s} \neq s)) P^{(I)}(\hat{s} \neq s). \quad (39)$$

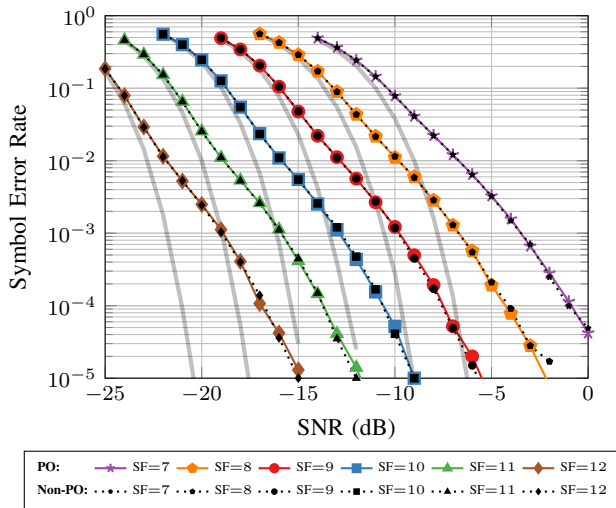


Fig. 2. Symbol error rate of the LoRa modulation under AWGN and same-SF interference for $SF \in \{7, \dots, 12\}$ and $P_I = -3$ dB.

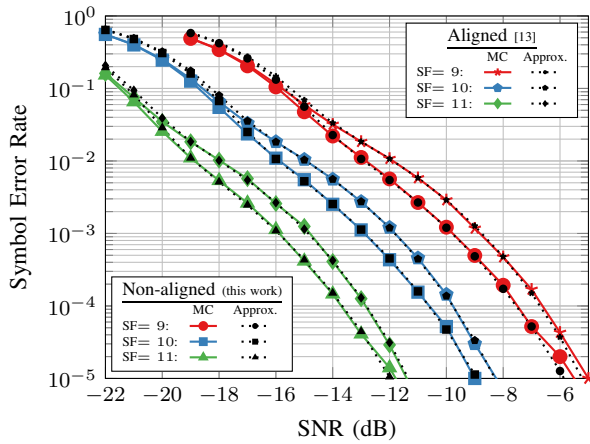


Fig. 3. Symbol error rate of the LoRa modulation under AWGN and same-SF interference for $SF \in \{9, 10, 11\}$ and $P_I = -3$ dB.

VI. RESULTS

In this section, we provide numerical results for the SER of a LoRa user with same-SF interference. In the remainder of this section, we use $\epsilon = 1/10$ to discretize the integral in (38).

In Fig. 2, we show the results of a Monte Carlo simulation for the SER of a LoRa user for all possible spreading factors $SF \in \{7, \dots, 12\}$, under the effect of same-SF interference with an SIR of 3 dB (i.e., $P_I = -3$ dB) and AWGN. The SER when there is only AWGN is also included in the figure with thick transparent lines. We can clearly observe the strong impact of the interference on the SER when comparing to the case where there is only AWGN. The black dotted lines in the figure depict the SER when the relative phase offset between the interferer and the user ω is not taken into account in the Monte Carlo simulation. It is interesting to observe that ω does not seem to play an important role for the SER, which further justifies ignoring ω in the approximation of Section V.

In Fig. 3, we show the results of a Monte Carlo simulation

for the SER of a LoRa user for $SF \in \{9, 10, 11\}$ using the chip-aligned model of [13] and the model we described in this work, as well as the corresponding approximations in [13] and (39), respectively. We observe that there is a significant difference of approximately 1 dB between the two models. The chip-aligned model of [13] is pessimistic in the computation of the SER. Finally, we clearly observe that the low-complexity computation of (18) using the approximation derived in Section V is very accurate.

VII. CONCLUSION

In this work, we introduced a LoRa interference model where the interference is neither chip- nor phase-aligned with the LoRa signal-of-interest and we derived a corresponding expression for the SER. Moreover, we derived a low-complexity approximation for the SER and we showed that ignoring the non-integer time offsets overestimates the error rate by 1 dB.

REFERENCES

- [1] Semtech Corporation, "SX1272/73-860 MHz to 1020 MHz low power long range transceiver." [Online]. Available: <https://www.semtech.com/uploads/documents/sx1272.pdf>
- [2] M. Knight and B. Seeber, "Decoding LoRa: Realizing a modern LPWAN with SDR," in *GNU Radio Conf.*, Sep. 2016.
- [3] P. Robyns, P. Quax, W. Lamotte, and W. Thenaers, "A multi-channel software decoder for the LoRa modulation scheme," in *Int. Conf. on Internet of Things, Big Data and Security (IoTBDS)*, Mar. 2018.
- [4] L. Vangelista, "Frequency shift chirp modulation: The LoRa modulation," *IEEE Signal Process. Lett.*, vol. 24, no. 12, pp. 1818-1821, Dec. 2017.
- [5] R. Ghanaatian, O. Afisiadis, M. Cotting, and A. Burg, "LoRa digital receiver analysis and implementation," *ArXiv e-prints*, Feb. 2019, <https://arxiv.org/abs/1811.04146>.
- [6] M. C. Bor, U. Roedig, T. Voigt, and J. M. Alonso, "Do LoRa low-power wide-area networks scale?" in *ACM Int. Conf. on Modeling, Analysis and Simulation of Wireless and Mobile Systems*, ser. MSWiM '16. New York, NY, USA: ACM, 2016, pp. 59-67.
- [7] J. Haxhibeqiri, E. De Poorter, I. Moerman, and J. Hoebeke, "A survey of LoRaWAN for IoT: From technology to application," *Sensors*, vol. 18, no. 11, 2018.
- [8] C. Orfanidis, L. M. Feeney, M. Jacobsson, and P. Gunningberg, "Investigating interference between LoRa and IEEE 802.15.4g networks," in *IEEE Int. Conf. on Wireless and Mobile Computing, Networking and Communications (WiMob)*, Oct. 2017, pp. 1-8.
- [9] B. Reynders, W. Meert, and S. Pollin, "Range and coexistence analysis of long range unlicensed communication," in *Int. Conf. on Telecommunications (ICT)*, May 2016, pp. 1-6.
- [10] D. Croce, M. Gucciardo, S. Mangione, G. Santaromita, and I. Tinnirello, "Impact of LoRa imperfect orthogonality: Analysis of link-level performance," *IEEE Commun. Lett.*, vol. 22, no. 4, pp. 796-799, Apr. 2018.
- [11] L. Feltrin, C. Buratti, E. Vinciarelli, R. De Bonis, and R. Verdone, "LoRaWAN: Evaluation of link- and system-level performance," *IEEE Internet of Things Journal*, vol. 5, no. 3, pp. 2249-2258, Jun. 2018.
- [12] T. Elshabrawy and J. Robert, "Closed-form approximation of LoRa modulation BER performance," *IEEE Commun. Lett.*, vol. 22, no. 9, pp. 1778-1781, Sep. 2018.
- [13] T. Elshabrawy and J. Robert, "Analysis of BER and coverage performance of LoRa modulation under same spreading factor interference," in *IEEE Int. Symp. on Personal, Indoor and Mobile Radio Communications (PIMRC)*, Sep. 2018.
- [14] T. Elshabrawy and J. Robert, "Capacity planning of LoRa networks with joint noise-limited and interference-limited coverage considerations," *IEEE Sensors Journal*, pp. 1-1, Feb. 2019.
- [15] H. A. David and H. N. Nagaraja, *Order Statistics*. Wiley, 2003.
- [16] F. Adelantado, X. Vilajosana, P. Tuset-Peiro, B. Martinez, J. Melia-Segui, and T. Watteyne, "Understanding the limits of LoRaWAN," *IEEE Commun. Mag.*, vol. 55, no. 9, pp. 34-40, Sep. 2017.
- [17] C. Goursaud and J.-M. Gorce, "Dedicated networks for IoT : PHY / MAC state of the art and challenges," *EAI endorsed trans. on Internet of Things*, Oct. 2015.